EUROPEAN ORGANIZATION FOR NUCLEAR RESEARCH

CERN-EP-2000-006
January 11, 2000

Measurement of the $e^+e^- \rightarrow Z\gamma\gamma$ Cross Section and Determination of Quartic Gauge Boson Couplings at LEP

The L3 Collaboration

Abstract

A first measurement of the cross section of the process $e^+e^- \rightarrow Z\gamma\gamma$ is reported using a total integrated luminosity of $231\,\mathrm{pb}^{-1}$ collected with the L3 detector at centre-of-mass energies of 182.7 GeV and 188.7 GeV. By selecting hadronic events with two isolated photons the $e^+e^- \rightarrow Z\gamma\gamma$ cross section is measured to be $0.49^{+0.20}_{-0.17} \pm 0.04\,\mathrm{pb}$ at 182.7 GeV and $0.47 \pm 0.10 \pm 0.04\,\mathrm{pb}$ at 188.7 GeV. The measurements are consistent with Standard Model expectations. Limits on Quartic Gauge Boson Couplings a_0/Λ^2 and a_c/Λ^2 of $-0.009\ \mathrm{GeV}^{-2} < a_0/\Lambda^2 < 0.008\ \mathrm{GeV}^{-2}$ and $-0.007\ \mathrm{GeV}^{-2} < a_c/\Lambda^2 < 0.013\ \mathrm{GeV}^{-2}$ are derived at 95% confidence level.

Submitted to *Phys. Lett. B*

1 Introduction

The LEP centre-of-mass energy ($\sqrt{s}$) for e^+e^- collisions has now exceeded the W pair and Z pair production thresholds, allowing the study of triple gauge boson production processes such as $e^+e^- \to Z\gamma\gamma$ and $e^+e^- \to W^+W^-\gamma$. Measurements of these processes give a new insight into the Standard Model of electroweak interactions (SM) [1]. The possibility of these triple gauge boson production processes proceeding via s-channel exchange of a fourth boson provides a probe of quartic gauge boson couplings (QGC). Such measurements were recently performed for the $e^+e^- \to W^+W^-\gamma$ process [2].

This letter describes the first measurement of the cross section of the process $e^+e^- \to Z\gamma\gamma$ followed by the hadronic decay of the Z. In the SM this process occurs by radiation of the photons from the incoming electron and/or positron, corresponding to a total of six diagrams, three of which are presented in Figure 1. No QGC contribution is predicted at the tree level and $Z\gamma\gamma$ events are sensitive to anomalous QGC [3–5] contributions, as shown in Figure 1.

The measurement uses data collected with the L3 detector [6] at LEP in 1997 and 1998 at average centre-of-mass energies of $\sqrt{s} = 182.7$ GeV and $\sqrt{s} = 188.7$ GeV corresponding to integrated luminosities of $55\,\mathrm{pb}^{-1}$ and $176\,\mathrm{pb}^{-1}$, respectively. These energies are respectively denoted as 183 GeV and 189 GeV hereafter.

The $e^+e^- \to Z\gamma\gamma \to q\bar{q}\gamma\gamma$ signal is defined by three phase space cuts: photon energies above 5 GeV, photon angles with respect to the beam axis between 14° and 166° and invariant mass of the primary produced quarks, before any radiation, within a $\pm 2\Gamma_Z$ window around the Z mass, Γ_Z being the Z width. The KK2f Monte Carlo (MC) program [7] predicts signal cross sections of about 0.4 pb at both energies.

2 Event Selection

The selection of events satisfying the signal definition given above is optimised using hadronic events generated at $\sqrt{s} = 189$ GeV with the KK2f MC program and at $\sqrt{s} = 183$ GeV with the PYTHIA 5.72 [8] MC program. Events from these MC programs failing the signal definition are termed QCD$\gamma\gamma$ background. Other background processes are generated both at $\sqrt{s} = 183$ GeV and $\sqrt{s} = 189$ GeV with the MC programs PYTHIA ($e^+e^- \to Ze^+e^-$ and $e^+e^- \to ZZ$), KORALZ 4.02 [9] ($e^+e^- \to \tau^+\tau^-(\gamma)$), PHOJET 1.05c [10] ($e^+e^- \to e^+e^-q\bar{q}$) and KORALW 1.21 [11] for W^+W^- production except for the $e\nu_e q\bar{q}'$ final states which are generated with EXCALIBUR [12]. Additional background sources are found to be negligible.

The L3 detector response is simulated using the GEANT 3.15 program [13], which takes into account the effects of energy loss, multiple scattering and showering in the detector. Time dependent detector inefficiencies, as measured in each data taking period, are reproduced in these simulations.

The selection of $e^+e^- \to Z\gamma\gamma \to q\bar{q}\gamma\gamma$ candidates from balanced hadronic events with two photons and little energy deposition at low polar angles is based on photon energies and angles together with the invariant mass of the hadronic system. The photon energy and angle criteria follow directly from the signal definition whereas the invariant mass of the hadronic system is required to be between 74 GeV and 116 GeV. The main background after these selection requirements is due to the radiation of two initial state photons with a hadronic system failing the Z signal definition criteria. The boost β_Z of the recoiling system to the photons, assuming its mass to be the nominal Z mass, is on average larger for these background events. Candidate events are hence required to have $\beta_Z < 0.64$ at $\sqrt{s} = 183$ GeV and $\beta_Z < 0.66$ at $\sqrt{s} = 189$ GeV.

Another class of background events is the so called radiative return to the Z, where a photon in the initial state is emitted, bringing the effective $\sqrt{s}$ to the Z resonance. A Z boson is then produced decaying into a hadronic system with an electromagnetic energy deposition (*e.g.* final state radiation, misidentified electron or unresolved π^0) faking the least energetic photon of the signal selection. These events are rejected by an upper bound on the energy E_1^γ of the most energetic photon and a lower bound on the angle ω between the least energetic photon and its closest jet. Numerically $E_1^\gamma < 67.6$ GeV at $\sqrt{s} = 183$ GeV and $E_1^\gamma < 70.7$ GeV at $\sqrt{s} = 189$ GeV with $\omega > 17°$ at both the energies.

Data and MC distributions of the selection variables are presented in Figure 2 for $\sqrt{s} = 189$ GeV, where selection criteria on all the other variables are applied. A good agreement between data and MC is observed.

3 Results and Systematic Uncertainties

The application of the selection procedure described above yields the signal efficiencies and selected data and MC events summarised in Table 1. A clear signal structure is observed in the recoil mass spectra of the two photons, presented in Figure 3 for the two centre-of-mass energies under study. The $e^+e^- \rightarrow Z\gamma\gamma \rightarrow q\bar{q}\gamma\gamma$ cross section at $\sqrt{s} = 183$ GeV and $\sqrt{s} = 189$ GeV is then determined from the number of events selected and the efficiency and background estimates from MC.

$\sqrt{s}$ (GeV)	183	189
ε	0.49	0.51
Data	12	36
MC	13.4	39.2
$Z\gamma\gamma$	10.6	32.6
QCD$\gamma\gamma$	2.7	6.0
Other	0.1	0.6

Table 1: Yields of the $e^+e^- \rightarrow Z\gamma\gamma \rightarrow q\bar{q}\gamma\gamma$ selection at $\sqrt{s} = 183$ GeV and $\sqrt{s} = 189$ GeV. The signal efficiencies ε and the number of expected events for data and MC are given.

Systematic uncertainties on the cross section measurements are listed in Table 2. They include uncertainties arising from the signal MC statistical error of 3% at $\sqrt{s} = 183$ GeV and 5% at $\sqrt{s} = 189$ GeV. The uncertainty on the accepted background due to MC statistics are 7% and 17% at $\sqrt{s} = 183$ GeV and $\sqrt{s} = 189$ GeV, respectively. The calorimeter energy scale uncertainty is estimated by varying electromagnetic energies by $\pm 1\%$ and hadronic energies by $\pm 2\%$. Selection procedure systematics are obtained from the effect of removing each of the selection criteria. From a comparison of the KK2f and PYTHIA cross sections for hadronic events with a hard photon, a $\pm 15\%$ uncertainty on the background normalisation is conservatively estimated and propagated to the measured cross section. Uncertainties on signal efficiencies are estimated by comparing KK2f with PYTHIA and GRACE [14] MC program predictions and are found to be negligible. As these MC programs treat radiation with different approaches, these procedures also cover uncertainties in initial and final state radiation. The systematic error assigned to the reweighting procedure at $\sqrt{s} = 183$ GeV is estimated by applying the procedure to a sample generated with PYTHIA at $\sqrt{s} = 189$ GeV and comparing the corresponding cross section result to the previous one.

Source of Systematics	$\Delta\sigma$ (pb) 183 GeV	$\Delta\sigma$ (pb) 189 GeV
MC Statistics	0.02	0.02
Energy scale	0.02	0.02
Selection procedure	0.01	0.01
Background normalisation	0.01	< 0.01
Reweighting procedure	0.01	-
Total	0.03	0.03

Table 2: Systematic uncertainties $\Delta\sigma$ on the $\mathrm{e^+e^-} \rightarrow \mathrm{Z}\gamma\gamma \rightarrow \mathrm{q\bar{q}}\gamma\gamma$ cross section at $\sqrt{s} = 183$ GeV and $\sqrt{s} = 189$ GeV.

The cross section results are:

$$\begin{aligned}
\sigma_{\mathrm{e^+e^-}\rightarrow\mathrm{Z}\gamma\gamma\rightarrow\mathrm{q\bar{q}}\gamma\gamma}(183\ \mathrm{GeV}) &= 0.34^{+0.14}_{-0.12} \pm 0.03\,\mathrm{pb} \quad (\mathrm{SM}\ \ 0.396 \pm 0.005\,\mathrm{pb}) \\
\sigma_{\mathrm{e^+e^-}\rightarrow\mathrm{Z}\gamma\gamma\rightarrow\mathrm{q\bar{q}}\gamma\gamma}(189\ \mathrm{GeV}) &= 0.33 \pm 0.07 \pm 0.03\,\mathrm{pb} \quad (\mathrm{SM}\ \ 0.365 \pm 0.003\,\mathrm{pb}),
\end{aligned}$$

where the first uncertainties are statistical and the second systematic. The values in parentheses denote the SM expectations calculated from the KK2f MC with its default set of input parameters. The error on the predictions is the quadratic sum of the MC statistical error and the theory uncertainty estimated as suggested in Reference [7]. The measurements are in good agreement with these predictions. These results are also presented in Figure 4 together with the expected evolution with $\sqrt{s}$ of the SM cross section.

Scaling the measured cross sections for the Z hadronic branching ratio gives the $\mathrm{e^+e^-} \rightarrow \mathrm{Z}\gamma\gamma$ cross section at $\sqrt{s} = 183$ GeV and $\sqrt{s} = 189$ GeV:

$$\begin{aligned}
\sigma_{\mathrm{e^+e^-}\rightarrow\mathrm{Z}\gamma\gamma}(183\ \mathrm{GeV}) &= 0.49^{+0.20}_{-0.17} \pm 0.04\,\mathrm{pb} \\
\sigma_{\mathrm{e^+e^-}\rightarrow\mathrm{Z}\gamma\gamma}(189\ \mathrm{GeV}) &= 0.47 \pm 0.10 \pm 0.04\,\mathrm{pb}.
\end{aligned}$$

4 Limits on Quartic Gauge Boson Couplings

Anomalous QGC contributions to $\mathrm{Z}\gamma\gamma$ production via the s-channel exchange of a Z are described by two additional terms of dimension six in the Lagrangian [3]:

$$\begin{aligned}
\mathcal{L}_6^0 &= -\frac{\pi\alpha}{4\Lambda^2} a_0 F_{\mu\nu} F^{\mu\nu} \vec{W}_\rho \cdot \vec{W}^\rho \\
\mathcal{L}_6^c &= -\frac{\pi\alpha}{4\Lambda^2} a_c F_{\mu\rho} F^{\mu\sigma} \vec{W}^\rho \cdot \vec{W}_\sigma,
\end{aligned}$$

where α is the electromagnetic coupling, $F_{\mu\nu}$ is the field strength tensor of the photon and $\vec{W}_\mu$ is the weak boson field. For $\mathrm{Z}\gamma\gamma$ the third component of $\vec{W}_\mu$, $Z_\mu/\cos\theta_W$, is relevant. The parameters a_0 and a_c describe the strength of the QGC and Λ represents the scale of the New Physics responsible for the coupling. $\mathcal{L}_6^0$ and $\mathcal{L}_6^c$ are separately C and P conserving and no CP violating operators contribute to the anomalous $\mathrm{ZZ}\gamma\gamma$ vertex. A more detailed description of QGC has recently appeared [5]. While indirect limits on the QGC were derived from precision measurements at the Z pole [15], studies of $\mathrm{Z}\gamma\gamma$ and $\mathrm{W^+W^-}\gamma$ production probe the quantities a_0/Λ^2 and a_c/Λ^2 in a direct way. The $\mathrm{e^+e^-} \rightarrow \mathrm{Z}\gamma\gamma$ process is expected to have higher sensitivities than $\mathrm{e^+e^-} \rightarrow \mathrm{W^+W^-}\gamma$. This is due to an extra factor of $1/\cos^4\theta_W$ in the QGC cross section, to the larger SM cross section and data statistics and to the smaller number of SM diagrams [4].

QGC are expected to manifest themselves via deviations in the total $\mathrm{e^+e^-} \rightarrow \mathrm{Z}\gamma\gamma$ cross section, as presented in Figure 4. As the $\mathrm{Z}\gamma\gamma$ production occurs in the SM via t-channel diagrams, the three body phase space favoured in the QGC mediated production is different, in particular resulting in a harder spectrum of the least energetic photon [5]. Figures 5a and 5b compare these reconstructed spectra with the predictions from signal and background MC at $\sqrt{s} = 183$ GeV and $\sqrt{s} = 189$ GeV. The expectations for an anomalous value of a_0/Λ^2 or a_c/Λ^2 are also shown. These QGC predictions are obtained by reweighting each SM signal MC event with the ratio $\mathcal{W}(\Omega, a_0/\Lambda^2, a_c/\Lambda^2)$, a function of its phase space Ω derived from the two photons and the Z mass and the values of the couplings:

$$\mathcal{W}(\Omega, a_0/\Lambda^2, a_c/\Lambda^2) = \frac{|\mathcal{M}_{SM}(\Omega) + \mathcal{M}_{QGC}(\Omega, a_0/\Lambda^2, a_c/\Lambda^2)|^2}{|\mathcal{M}_{SM}(\Omega)|^2}.$$

$\mathcal{M}_{SM}$ denotes the SM matrix element and $\mathcal{M}_{QGC}$ the QGC one, both calculated analytically [4]. Possible extra initial state photons are taken into account in the calculation of Ω.

A simultaneous fit to the two energy spectra is performed leaving one of the two QGC free at a time, fixing the other to zero. The SM predictions in the fit procedure are reweighted as described above, yielding the 68% confidence level (CL) measurements:

$$a_0/\Lambda^2 = 0.001 \pm 0.004 \text{ GeV}^{-2} \text{ and } a_c/\Lambda^2 = 0.003 \pm 0.005 \text{ GeV}^{-2},$$

in agreement with the expected SM value of zero. A simultaneous fit to both the parameters yields the 95% CL limits:

$$-0.009 \text{ GeV}^{-2} < a_0/\Lambda^2 < 0.008 \text{ GeV}^{-2} \text{ and } -0.007 \text{ GeV}^{-2} < a_c/\Lambda^2 < 0.013 \text{ GeV}^{-2},$$

as shown in Figure 6. A correlation of -35% is observed. The experimental systematic uncertainties and those on the SM $\mathrm{e^+e^-} \rightarrow \mathrm{Z}\gamma\gamma \rightarrow \mathrm{q\bar{q}}\gamma\gamma$ cross section predictions are taken into account.

Acknowledgements

We are indebted to Anja Werthenbach for providing us with the $\mathrm{e^+e^-} \rightarrow \mathrm{Z}\gamma\gamma$ analytical calculations and for the inspiring discussions. We wish to express our gratitude to the CERN accelerator divisions for the superb performance and the continuous and successful upgrade of the LEP machine. We acknowledge the contributions of the engineers and technicians who have participated in the construction and maintenance of this experiment.

References

[1] S. L. Glashow, Nucl. Phys. **22** (1961) 579; A. Salam, in Elementary Particle Theory, ed. N. Svartholm, (Almqvist and Wiksell, Stockholm, 1968), p. 367; S. Weinberg, Phys. Rev. Lett. **19** (1967) 1264.

[2] OPAL Collab., G. Abbiendi *et al.*, Phys. Lett. **B 471** (1999) 293.

[3] G. Bélanger and F. Boudjema, Phys. Lett. **B 288** (1992) 201.

[4] W. J. Stirling and A. Werthenbach, Preprint DTP/99/30, hep-ph/9903315.

[5] G. Bélanger *et al.*, Preprint LAPTH-744/19, hep-ph/9908254.

[6] L3 Collab., B. Adeva *et al.*, Nucl. Inst. Meth. **A 289** (1990) 35; L3 Collab., O. Adriani *et al.*, Physics Reports **236** (1993) 1; I. C. Brock *et al.*, Nucl. Instr. and Meth. **A 381** (1996) 236; M. Chemarin *et al.*, Nucl. Inst. Meth. **A 349** (1994) 345; M. Acciarri *et al.*, Nucl. Inst. Meth. **A 351** (1994) 300; A. Adam *et al.*, Nucl. Inst. Meth. **A 383** (1996) 342; G. Basti *et al.*, Nucl. Inst. Meth. **A 374** (1996) 293.

[7] S. Jadach, B.F.L. Ward and Z. Wąs, Preprint CERN-TH/99-235, hep-ph/9912214.

[8] T. Sjöstrand, CERN–TH/7112/93 (1993), revised August 1995; T. Sjöstrand, Comp. Phys. Comm. **82** (1994) 74.

[9] S. Jadach, B. F. L. Ward and Z. Wąs, Comp. Phys. Comm **79** (1994) 503.

[10] R. Engel, Z. Phys. **C 66** (1995) 203; R. Engel and J. Ranft, Phys. Rev. **D 54** (1996) 4244.

[11] M. Skrzypek *et al.*, Comp. Phys. Comm. **94** (1996) 216; M. Skrzypek *et al.*, Phys. Lett. **B 372** (1996) 289.

[12] R. Kleiss and R. Pittau, Comp. Phys. Comm. **85** (1995) 447; R. Pittau, Phys. Lett. **B 335** (1994) 490.

[13] The L3 detector simulation is based on GEANT Version 3.15. R. Brun *et al.*, "GEANT 3", CERN–DD/EE/84–1 (Revised), 1987. The GHEISHA program (H. Fesefeldt, RWTH Aachen Report PITHA 85/02 (1985)) is used to simulate hadronic interactions.

[14] T. Ishikawa *et al.*, KEK Report 92-19.

[15] A. Brunstein, O. J. P. Éboli and M. C. Gonzales-Garcia, Phys. Lett. **B 375** (1996) 233.

The L3 Collaboration:

M.Acciarri,[26] P.Achard,[19] O.Adriani,[16] M.Aguilar-Benitez,[25] J.Alcaraz,[25] G.Alemanni,[22] J.Allaby,[17] A.Aloisio,[28] M.G.Alviggi,[28] G.Ambrosi,[19] H.Anderhub,[48] V.P.Andreev,[6,36] T.Angelescu,[12] F.Anselmo,[9] A.Arefiev,[27] T.Azemoon,[3] T.Aziz,[10] P.Bagnaia,[35] L.Baksay,[43] A.Balandras,[4] R.C.Ball,[3] S.Banerjee,[10] Sw.Banerjee,[10] A.Barczyk,[48,46] R.Barillère,[17] L.Barone,[35] P.Bartalini,[22] M.Basile,[9] R.Battiston,[32] A.Bay,[22] F.Becattini,[16] U.Becker,[14] F.Behner,[48] L.Bellucci,[16] J.Berdugo,[25] P.Berges,[14] B.Bertucci,[32] B.L.Betev,[48] S.Bhattacharya,[10] M.Biasini,[32] M.Biglietti,[28] A.Biland,[48] J.J.Blaising,[4] S.C.Blyth,[33] G.J.Bobbink,[2] A.Böhm,[1] L.Boldizsar,[13] B.Borgia,[35] D.Bourilkov,[48] M.Bourquin,[19] S.Braccini,[19] J.G.Branson,[39] V.Brigljevic,[48] F.Brochu,[4] A.Buffini,[16] A.Buijs,[44] J.D.Burger,[14] W.J.Burger,[32] A.Button,[3] X.D.Cai,[14] M.Campanelli,[48] M.Capell,[14] G.Cara Romeo,[9] G.Carlino,[28] A.M.Cartacci,[16] J.Casaus,[25] G.Castellini,[16] F.Cavallari,[35] N.Cavallo,[37] C.Cecchi,[32] M.Cerrada,[25] F.Cesaroni,[23] M.Chamizo,[19] Y.H.Chang,[50] U.K.Chaturvedi,[18] M.Chemarin,[24] A.Chen,[50] G.Chen,[7] G.M.Chen,[7] H.F.Chen,[20] H.S.Chen,[7] G.Chiefari,[28] L.Cifarelli,[38] F.Cindolo,[9] C.Civinini,[16] I.Clare,[14] R.Clare,[14] G.Coignet,[4] A.P.Colijn,[2] N.Colino,[25] S.Costantini,[5] F.Cotorobai,[12] B.Cozzoni,[9] B.de la Cruz,[25] A.Csilling,[13] S.Cucciarelli,[32] T.S.Dai,[14] J.A.van Dalen,[30] R.D'Alessandro,[16] R.de Asmundis,[28] P.Déglon,[19] A.Degré,[4] K.Deiters,[46] D.della Volpe,[28] P.Denes,[34] F.DeNotaristefani,[35] A.De Salvo,[48] M.Diemoz,[35] D.van Dierendonck,[2] F.Di Lodovico,[48] C.Dionisi,[35] M.Dittmar,[48] A.Dominguez,[39] A.Doria,[28] M.T.Dova,[18,♯] D.Duchesneau,[4] D.Dufournaud,[4] P.Duinker,[2] I.Duran,[40] H.El Mamouni,[24] A.Engler,[33] F.J.Eppling,[14] F.C.Erné,[2] P.Extermann,[19] M.Fabre,[46] R.Faccini,[35] M.A.Falagan,[25] S.Falciano,[35,17] A.Favara,[17] J.Fay,[24] O.Fedin,[36] M.Felcini,[48] T.Ferguson,[33] F.Ferroni,[35] H.Fesefeldt,[1] E.Fiandrini,[32] J.H.Field,[19] F.Filthaut,[17] P.H.Fisher,[14] I.Fisk,[39] G.Forconi,[14] L.Fredj,[19] K.Freudenreich,[48] C.Furetta,[26] Yu.Galaktionov,[27,14] S.N.Ganguli,[10] P.Garcia-Abia,[5] M.Gataullin,[31] S.S.Gau,[11] S.Gentile,[35,17] N.Gheordanescu,[12] S.Giagu,[35] Z.F.Gong,[20] G.Grenier,[24] O.Grimm,[48] M.W.Gruenewald,[8] M.Guida,[38] R.van Gulik,[2] V.K.Gupta,[34] A.Gurtu,[10] L.J.Gutay,[45] D.Haas,[5] A.Hasan,[29] D.Hatzifotiadou,[9] T.Hebbeker,[8] A.Hervé,[17] P.Hidas,[13] J.Hirschfelder,[33] H.Hofer,[48] G. Holzner,[48] H.Hoorani,[33] S.R.Hou,[50] I.Iashvili,[47] B.N.Jin,[7] L.W.Jones,[3] P.de Jong,[2] I.Josa-Mutuberría,[25] R.A.Khan,[18] M.Kaur,[18,◇] M.N.Kienzle-Focacci,[19] D.Kim,[35] D.H.Kim,[42] J.K.Kim,[42] S.C.Kim,[42] J.Kirkby,[17] D.Kiss,[13] W.Kittel,[30] A.Klimentov,[14,27] A.C.König,[30] A.Kopp,[47] V.Koutsenko,[14,27] M.Kräber,[48] R.W.Kraemer,[33] W.Krenz,[1] A.Krüger,[47] A.Kunin,[14,27] P.Ladron de Guevara,[25] I.Laktineh,[24] G.Landi,[16] K.Lassila-Perini,[48] M.Lebeau,[17] A.Lebedev,[14] P.Lebrun,[24] P.Lecomte,[48] P.Lecoq,[17] P.Le Coultre,[48] H.J.Lee,[8] J.M.Le Goff,[17] R.Leiste,[47] E.Leonardi,[35] P.Levtchenko,[36] C.Li,[20] S.Likhoded,[47] C.H.Lin,[50] W.T.Lin,[50] F.L.Linde,[2] L.Lista,[28] Z.A.Liu,[7] W.Lohmann,[47] E.Longo,[35] Y.S.Lu,[7] K.Lübelsmeyer,[1] C.Luci,[17,35] D.Luckey,[14] L.Lugnier,[24] L.Luminari,[35] W.Lustermann,[48] W.G.Ma,[20] M.Maity,[10] L.Malgeri,[17] A.Malinin,[17] C.Maña,[25] D.Mangeol,[30] P.Marchesini,[48] G.Marian,[15] J.P.Martin,[24] F.Marzano,[35] G.G.G.Massaro,[2] K.Mazumdar,[10] R.R.McNeil,[6] S.Mele,[17] L.Merola,[28] M.Meschini,[16] W.J.Metzger,[30] M.von der Mey,[1] A.Mihul,[12] H.Milcent,[17] G.Mirabelli,[35] J.Mnich,[17] G.B.Mohanty,[10] P.Molnar,[8] B.Monteleoni,[16,†] T.Moulik,[10] G.S.Muanza,[24] F.Muheim,[19] A.J.M.Muijs,[2] M.Musy,[35] M.Napolitano,[28] F.Nessi-Tedaldi,[48] H.Newman,[31] T.Niessen,[1] A.Nisati,[35] H.Nowak,[47] Y.D.Oh,[42] G.Organtini,[35] A.Oulianov,[27] C.Palomares,[25] D.Pandoulas,[1] S.Paoletti,[35,17] P.Paolucci,[28] R.Paramatti,[35] H.K.Park,[33] I.H.Park,[42] G.Pascale,[35] G.Passaleva,[17] S.Patricelli,[28] T.Paul,[11] M.Pauluzzi,[32] C.Paus,[17] F.Pauss,[48] M.Pedace,[35] S.Pensotti,[26] D.Perret-Gallix,[4] B.Petersen,[30] D.Piccolo,[28] F.Pierella,[9] M.Pieri,[16] P.A.Piroué,[34] E.Pistolesi,[26] V.Plyaskin,[27] M.Pohl,[19] V.Pojidaev,[27,16] H.Postema,[14] J.Pothier,[17] N.Produit,[19] D.O.Prokofiev,[45] D.Prokofiev,[36] J.Quartieri,[38] G.Rahal-Callot,[48,17] M.A.Rahaman,[10] P.Raics,[15] N.Raja,[10] R.Ramelli,[48] P.G.Rancoita,[26] A.Raspereza,[47] G.Raven,[39] P.Razis,[29] D.Ren,[48] M.Rescigno,[35] S.Reucroft,[11] T.van Rhee,[44] S.Riemann,[47] K.Riles,[3] A.Robohm,[48] J.Rodin,[43] B.P.Roe,[3] L.Romero,[25] A.Rosca,[8] S.Rosier-Lees,[4] J.A.Rubio,[17] D.Ruschmeier,[8] H.Rykaczewski,[48] S.Saremi,[6] S.Sarkar,[35] J.Salicio,[17] E.Sanchez,[17] M.P.Sanders,[30] M.E.Sarakinos,[21] C.Schäfer,[17] V.Schegelsky,[36] S.Schmidt-Kaerst,[1] D.Schmitz,[1] H.Schopper,[49] D.J.Schotanus,[30] G.Schwering,[1] C.Sciacca,[28] D.Sciarrino,[19] A.Seganti,[9] L.Servoli,[32] S.Shevchenko,[31] N.Shivarov,[41] V.Shoutko,[27] E.Shumilov,[27] A.Shvorob,[31] T.Siedenburg,[1] D.Son,[42] B.Smith,[33] P.Spillantini,[16] M.Steuer,[14] D.P.Stickland,[34] A.Stone,[6] H.Stone,[34,†] B.Stoyanov,[41] A.Straessner,[1] K.Sudhakar,[10] G.Sultanov,[18] L.Z.Sun,[20] H.Suter,[48] J.D.Swain,[18] Z.Szillasi,[43,¶] T.Sztaricskai,[43,¶] X.W.Tang,[7] L.Tauscher,[5] L.Taylor,[11] C.Timmermans,[30] Samuel C.C.Ting,[14] S.M.Ting,[14] S.C.Tonwar,[10] J.Tóth,[13] C.Tully,[17] K.L.Tung,[7] Y.Uchida,[14] J.Ulbricht,[48] E.Valente,[35] G.Vesztergombi,[13] I.Vetlitsky,[27] D.Vicinanza,[38] G.Viertel,[48] S.Villa,[11] M.Vivargent,[4] S.Vlachos,[5] I.Vodopianov,[36] H.Vogel,[33] H.Vogt,[47] I.Vorobiev,[27] A.A.Vorobyov,[36] A.Vorvolakos,[29] M.Wadhwa,[5] W.Wallraff,[1] M.Wang,[14] X.L.Wang,[20] Z.M.Wang,[20] A.Weber,[1] M.Weber,[1] P.Wienemann,[1] H.Wilkens,[30] S.X.Wu,[14] S.Wynhoff,[17] L.Xia,[31] Z.Z.Xu,[20] B.Z.Yang,[20] C.G.Yang,[7] H.J.Yang,[7] M.Yang,[7] J.B.Ye,[20] S.C.Yeh,[51] An.Zalite,[36] Yu.Zalite,[36] Z.P.Zhang,[20] G.Y.Zhu,[7] R.Y.Zhu,[31] A.Zichichi,[9,17,18] G.Zilizi,[43,¶] M.Zöller.[1]

1 I. Physikalisches Institut, RWTH, D-52056 Aachen, FRG[§]
III. Physikalisches Institut, RWTH, D-52056 Aachen, FRG[§]
2 National Institute for High Energy Physics, NIKHEF, and University of Amsterdam, NL-1009 DB Amsterdam, The Netherlands
3 University of Michigan, Ann Arbor, MI 48109, USA
4 Laboratoire d'Annecy-le-Vieux de Physique des Particules, LAPP,IN2P3-CNRS, BP 110, F-74941 Annecy-le-Vieux CEDEX, France
5 Institute of Physics, University of Basel, CH-4056 Basel, Switzerland
6 Louisiana State University, Baton Rouge, LA 70803, USA
7 Institute of High Energy Physics, IHEP, 100039 Beijing, China[△]
8 Humboldt University, D-10099 Berlin, FRG[§]
9 University of Bologna and INFN-Sezione di Bologna, I-40126 Bologna, Italy
10 Tata Institute of Fundamental Research, Bombay 400 005, India
11 Northeastern University, Boston, MA 02115, USA
12 Institute of Atomic Physics and University of Bucharest, R-76900 Bucharest, Romania
13 Central Research Institute for Physics of the Hungarian Academy of Sciences, H-1525 Budapest 114, Hungary[‡]
14 Massachusetts Institute of Technology, Cambridge, MA 02139, USA
15 KLTE-ATOMKI, H-4010 Debrecen, Hungary[¶]
16 INFN Sezione di Firenze and University of Florence, I-50125 Florence, Italy
17 European Laboratory for Particle Physics, CERN, CH-1211 Geneva 23, Switzerland
18 World Laboratory, FBLJA Project, CH-1211 Geneva 23, Switzerland
19 University of Geneva, CH-1211 Geneva 4, Switzerland
20 Chinese University of Science and Technology, USTC, Hefei, Anhui 230 029, China[△]
21 SEFT, Research Institute for High Energy Physics, P.O. Box 9, SF-00014 Helsinki, Finland
22 University of Lausanne, CH-1015 Lausanne, Switzerland
23 INFN-Sezione di Lecce and Universitá Degli Studi di Lecce, I-73100 Lecce, Italy
24 Institut de Physique Nucléaire de Lyon, IN2P3-CNRS,Université Claude Bernard, F-69622 Villeurbanne, France
25 Centro de Investigaciones Energéticas, Medioambientales y Tecnologícas, CIEMAT, E-28040 Madrid, Spain♭
26 INFN-Sezione di Milano, I-20133 Milan, Italy
27 Institute of Theoretical and Experimental Physics, ITEP, Moscow, Russia
28 INFN-Sezione di Napoli and University of Naples, I-80125 Naples, Italy
29 Department of Natural Sciences, University of Cyprus, Nicosia, Cyprus
30 University of Nijmegen and NIKHEF, NL-6525 ED Nijmegen, The Netherlands
31 California Institute of Technology, Pasadena, CA 91125, USA
32 INFN-Sezione di Perugia and Universitá Degli Studi di Perugia, I-06100 Perugia, Italy
33 Carnegie Mellon University, Pittsburgh, PA 15213, USA
34 Princeton University, Princeton, NJ 08544, USA
35 INFN-Sezione di Roma and University of Rome, "La Sapienza", I-00185 Rome, Italy
36 Nuclear Physics Institute, St. Petersburg, Russia
37 INFN-Sezione di Napoli and University of Potenza, I-85100 Potenza, Italy
38 University and INFN, Salerno, I-84100 Salerno, Italy
39 University of California, San Diego, CA 92093, USA
40 Dept. de Fisica de Particulas Elementales, Univ. de Santiago, E-15706 Santiago de Compostela, Spain
41 Bulgarian Academy of Sciences, Central Lab. of Mechatronics and Instrumentation, BU-1113 Sofia, Bulgaria
42 Center for High Energy Physics, Adv. Inst. of Sciences and Technology, 305-701 Taejon, Republic of Korea
43 University of Alabama, Tuscaloosa, AL 35486, USA
44 Utrecht University and NIKHEF, NL-3584 CB Utrecht, The Netherlands
45 Purdue University, West Lafayette, IN 47907, USA
46 Paul Scherrer Institut, PSI, CH-5232 Villigen, Switzerland
47 DESY, D-15738 Zeuthen, FRG
48 Eidgenössische Technische Hochschule, ETH Zürich, CH-8093 Zürich, Switzerland
49 University of Hamburg, D-22761 Hamburg, FRG
50 National Central University, Chung-Li, Taiwan, China
51 Department of Physics, National Tsing Hua University, Taiwan, China
§ Supported by the German Bundesministerium für Bildung, Wissenschaft, Forschung und Technologie
‡ Supported by the Hungarian OTKA fund under contract numbers T019181, F023259 and T024011.
¶ Also supported by the Hungarian OTKA fund under contract numbers T22238 and T026178.
♭ Supported also by the Comisión Interministerial de Ciencia y Tecnología.
♯ Also supported by CONICET and Universidad Nacional de La Plata, CC 67, 1900 La Plata, Argentina.
◇ Also supported by Panjab University, Chandigarh-160014, India.
△ Supported by the National Natural Science Foundation of China.
† Deceased.

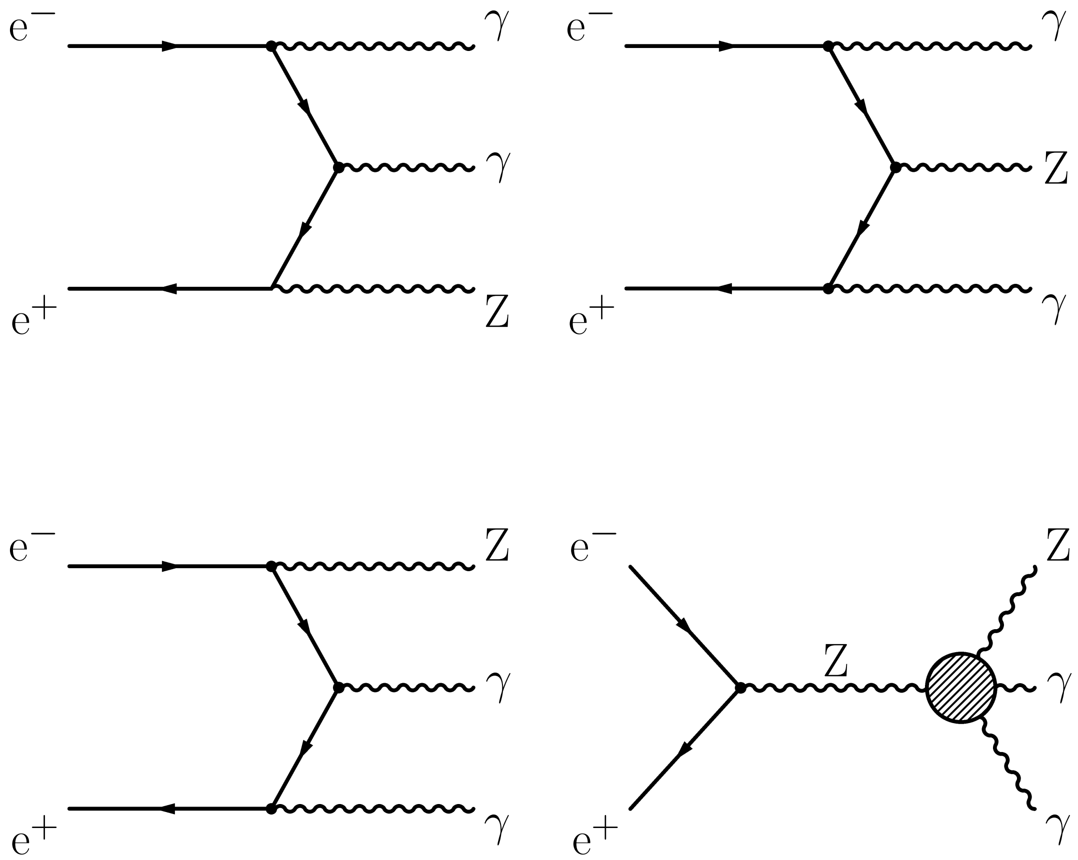

Figure 1: Three of the six SM diagrams contributing to $e^+e^- \rightarrow Z\gamma\gamma$ production. The other three SM diagrams are obtained by crossing the photon lines. A possible anomalous QGC diagram is also shown.

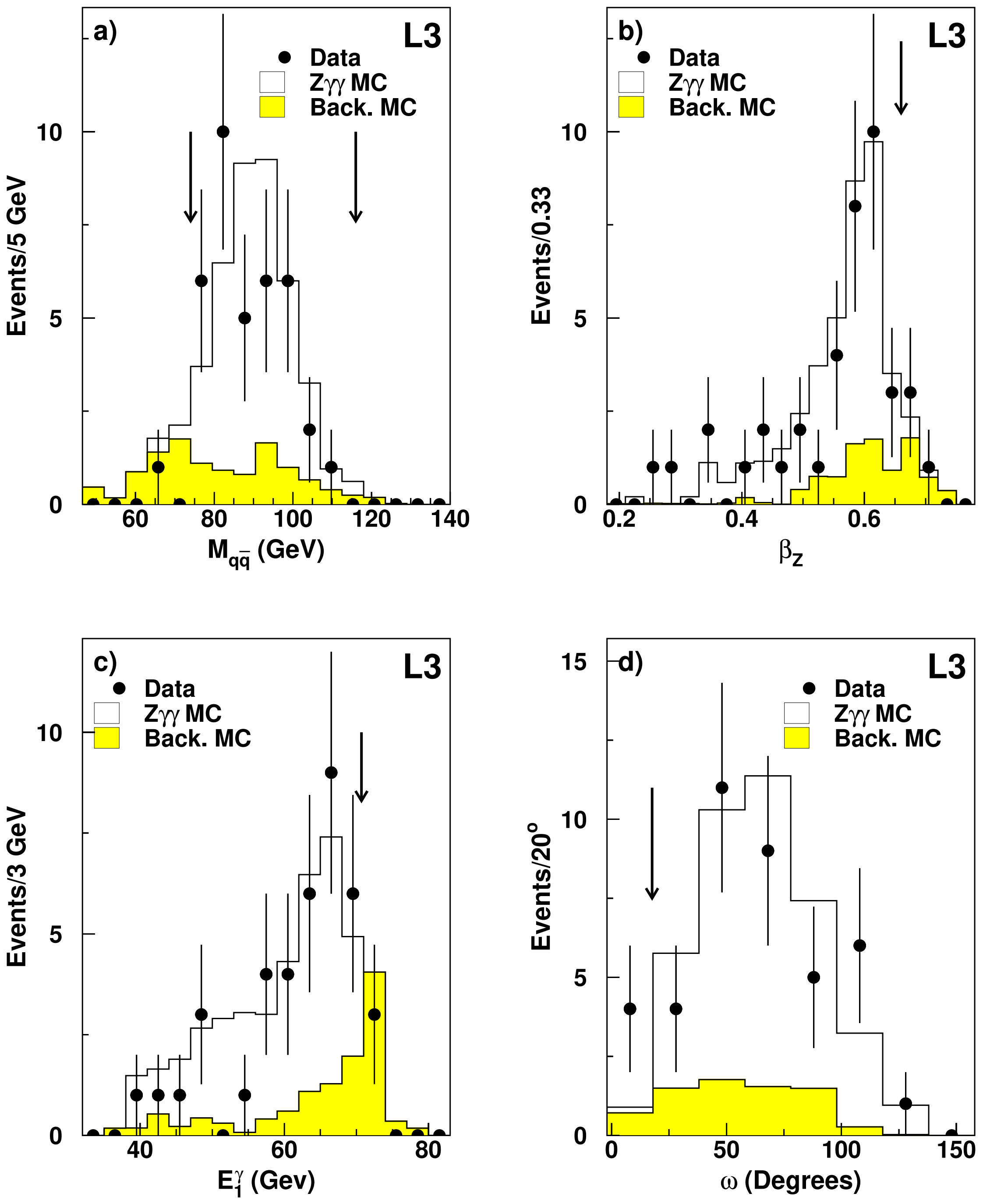

Figure 2: Distributions of (a) the invariant mass $M_{q\bar{q}}$ of the hadronic system, (b) the boost β_Z of the reconstructed Z boson, (c) the energy E_1^γ of the most energetic photon and (d) the angle ω between the least energetic photon and the nearest jet. Data, $Z\gamma\gamma$ and background MC are displayed for $\sqrt{s} = 189$ GeV. The arrows show the position of the final selection requirements. All the other selection criteria are applied for each plot.

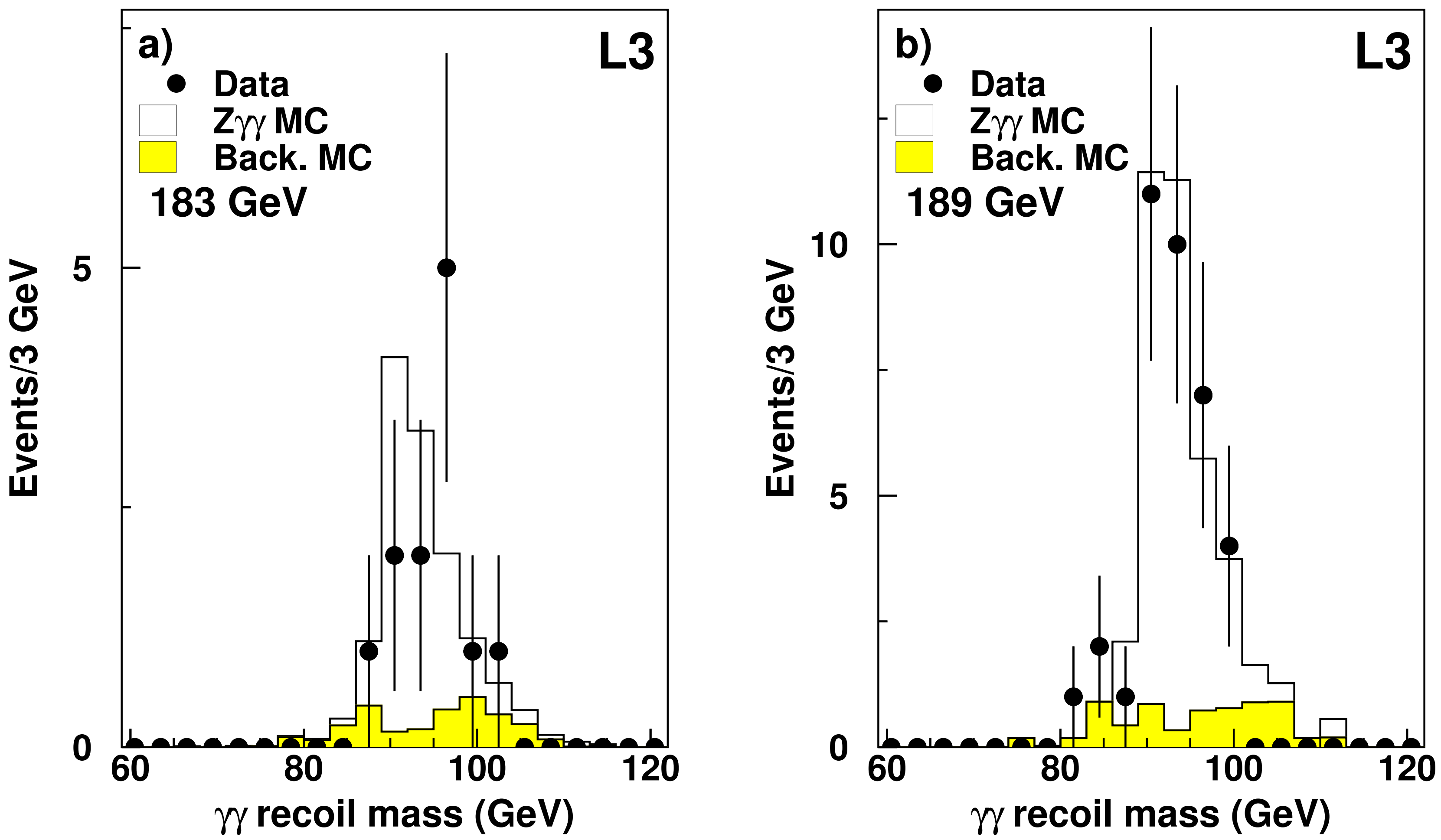

Figure 3: Recoil mass to the photon pairs at (a) $\sqrt{s}$ = 183 GeV and (b) $\sqrt{s}$ = 189 GeV in data, $Z\gamma\gamma$ and background MC.

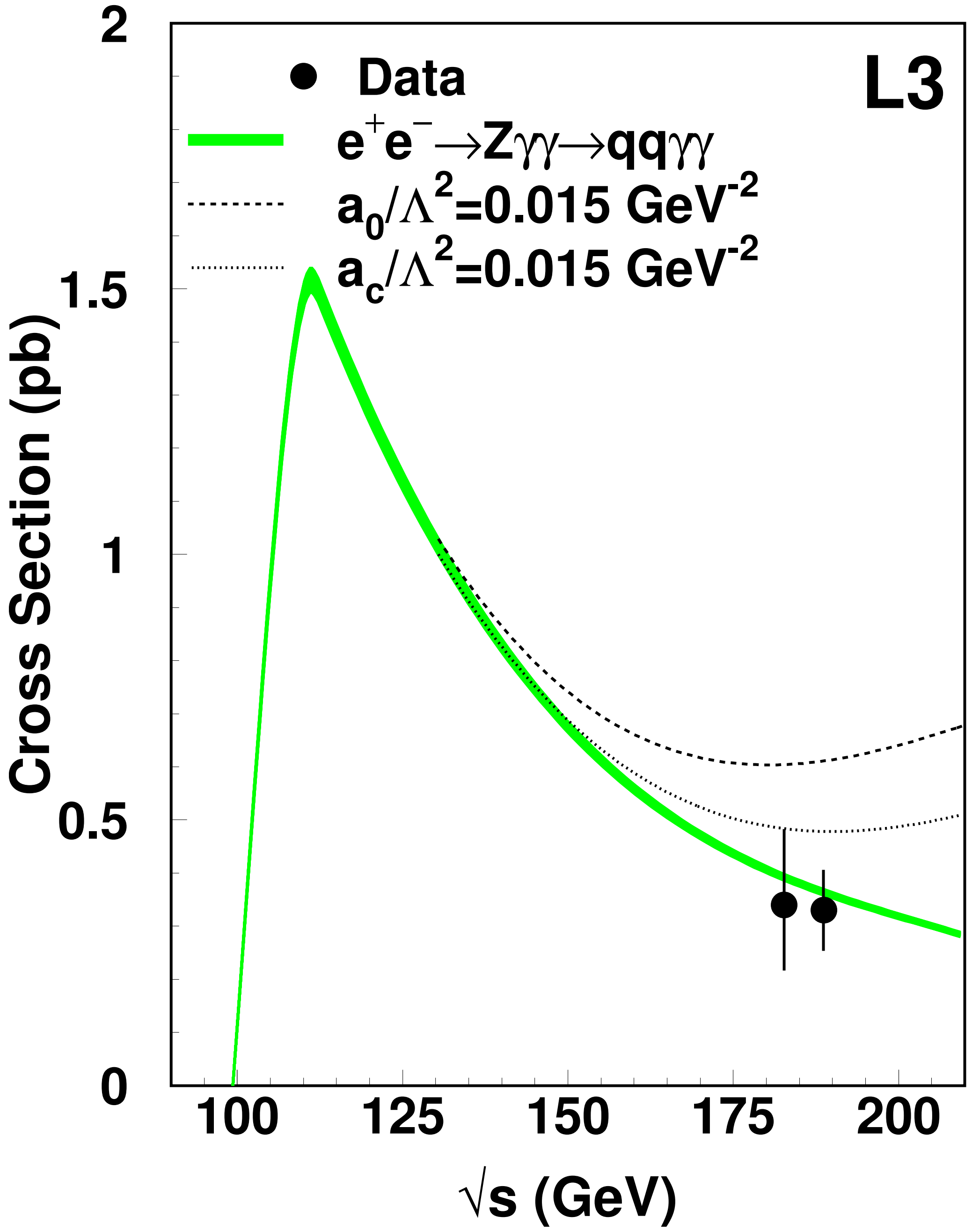

Figure 4: Evolution of the $e^+e^- \rightarrow Z\gamma\gamma \rightarrow q\bar{q}\gamma\gamma$ cross section with the centre-of-mass energy. Signal definition cuts described in the text are applied. The width of the band corresponds to the error that arises from MC statistics and theory uncertainty, estimated to be 1.5%. Dashed and dotted lines represent QGC predictions.

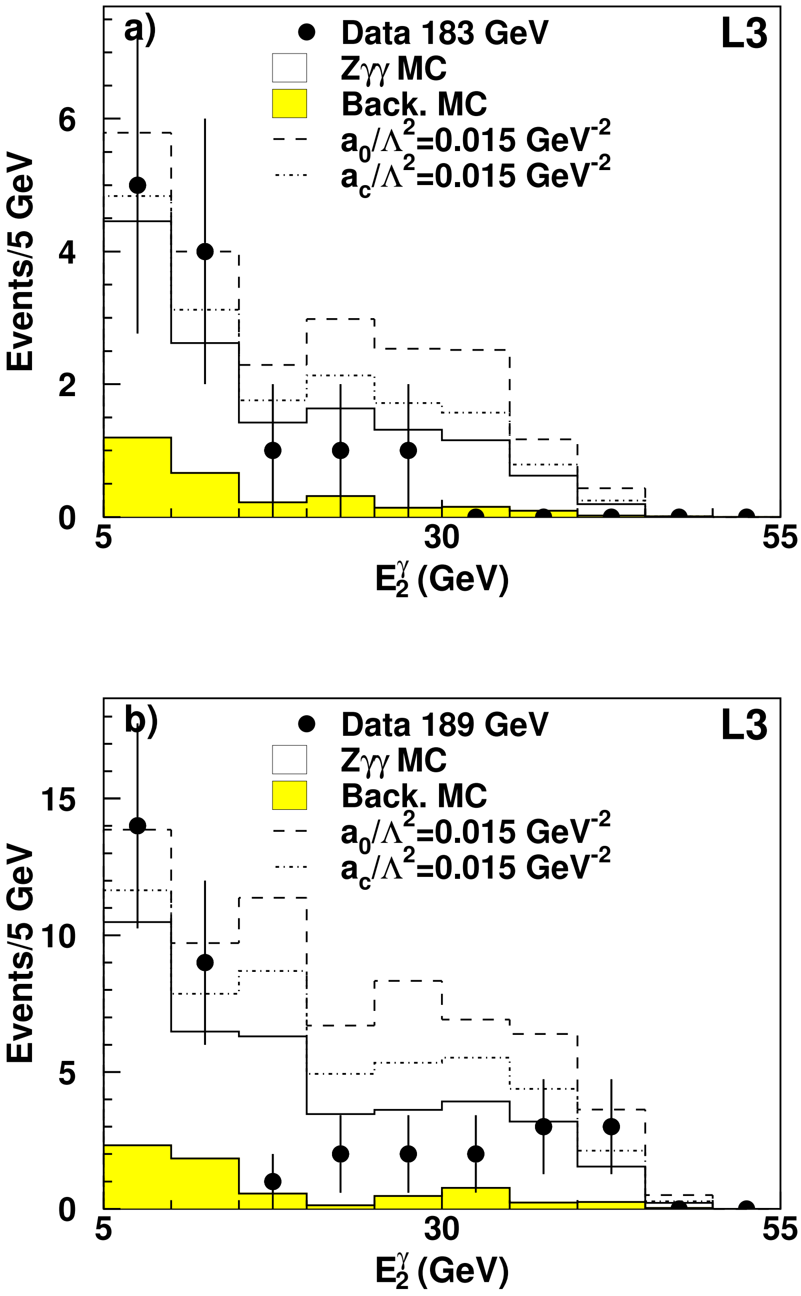

Figure 5: Energy E_2^γ of the least energetic photon for (a) $\sqrt{s}$ = 183 GeV and (b) $\sqrt{s}$ = 189 GeV. Data, $Z\gamma\gamma$ and background MC are displayed together with QGC predictions.

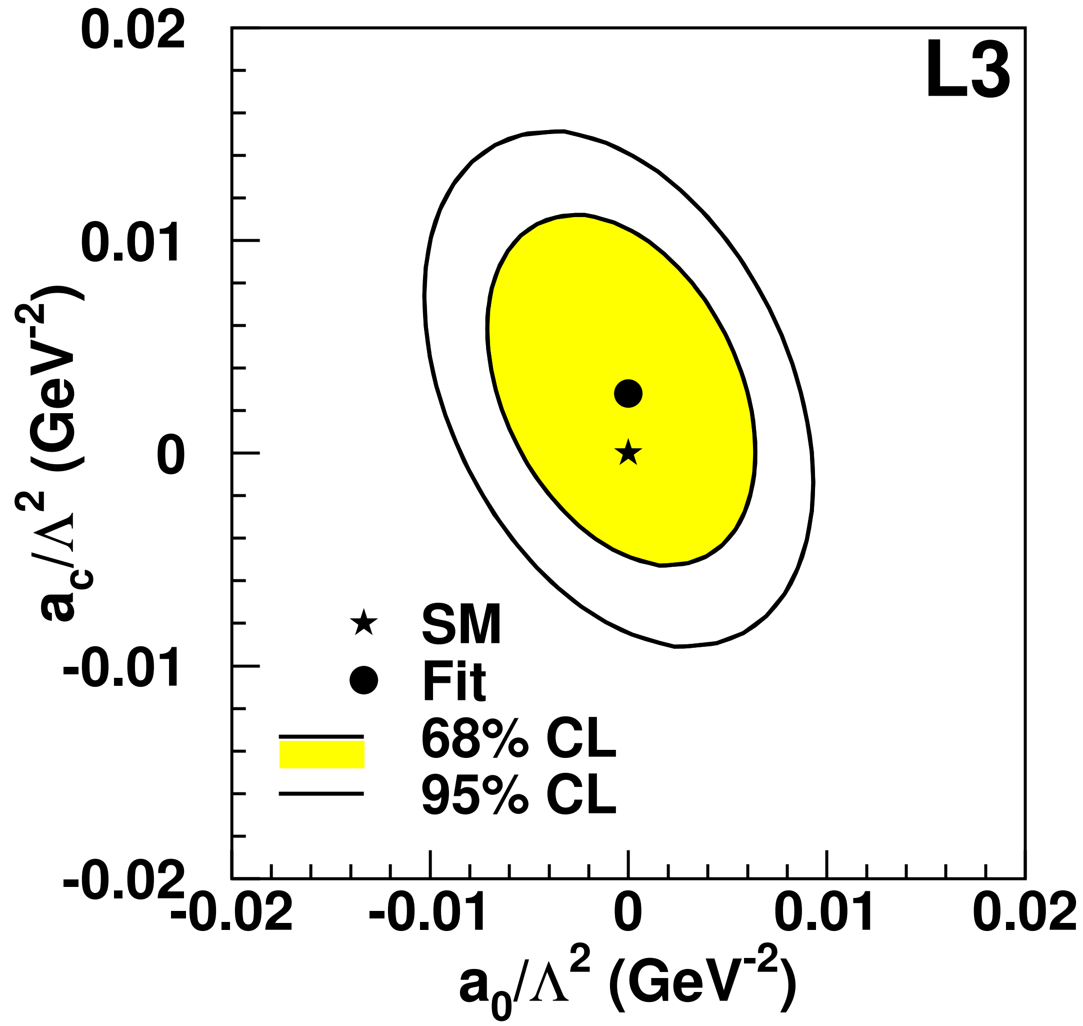

Figure 6: Two dimensional contours for the QGC parameters a_0/Λ^2 and a_c/Λ^2.